THE NEW C BAND GUN FOR THE NEXT GENERATION RF PHOTO-INJECTORS

D. Alesini, F. Cardelli, G. Di Raddo, L. Faillace, M. Ferrario, A. Gallo, A. Giribono, A. Gizzi,
S. Lauciani, A. Liedl, L. Pellegrino, L. Piersanti, C. Vaccarezza and A. Vannozzi
INFN-LNF, Frascati, Italy
M. Croia, ENEA, Casaccia, Italy
G. Castorina, AVO-ADAM, Meyrin, Switzerland
L. Ficcadenti and G. Pedrocchi, INFN Roma, Italy

Abstract

Rf photo-injectors are widely used in modern facilities, especially in FEL, as very low-emittance and high-brightness electron sources. Presently, the rf technology mostly used for guns is the S band (3 GHz) with typical cathode peak fields of 80-120 MV/m and repetition rates lower than 120 Hz. There are solid reasons to believe that the frequency step-up from S band to C band (~6 GHz) can provide a strong improvement of the beam quality due to the potential higher achievable cathode field (>160 MV/m) and higher repetition rate (that can reach the kHz level). In the contest of the European I.FAST project, a new C band gun has been designed and will be realized and tested. It is a 2.5 cell standing wave cavity with a four port mode launcher, designed to operate with short rf pulses (300 ns) and cathode peak field larger than 160 MV/m. In the paper we present the electromagnetic and thermo-mechanical design and the results of the prototyping activity with preliminary rf measurements.

INTRODUCTION

In the context of the X-band linacs of the EuPRAXIA@SPARC_LAB project [1] and XLS design study [2] the possibility to implement a full C-band injector is attractive for both the reachable beam parameters and compactness than for the possibility to operate at high repetition rate (up to 1 kHz). Since the peak field at the cathode (E_{cath}) is proportional to the achievable beam brightness [3], in the last generation of rf guns a great effort has been put to increase the field amplitude, and, at the same time, to reduce the breakdown rate probability (BDR) [4]. On the other hand, the possibility to operate such a gun at the kHz regime is very attractive for all mentioned projects. The realization and test of a C Band gun has been also funded by the EU in the framework of the I.FAST project [5] and by INFN Commission V. The gun, after its realization will be tested at PSI, Switzerland. In the present paper we illustrate the electromagnetic (e.m.) and thermo-mechanical design of the gun and the results of the prototyping activity. The gun is also attractive for its possible applications in upgrades of existing photo-injectors for FEL [6].

DESIGN CRITERIA OF THE GUN

The gun is a 2.5 cell structure and, as illustrated in [7], its design has been optimized in order to minimize the peak E field (E_{cath}), the modified Poynting vector (S_c) [8], the rf

pulse length (t_p) and pulsed heating (ΔT) [9]. The gun has been designed with a coupling coefficient equal to 3 to allow operation with short rf pulses (300 ns) thus reducing the BDR, pulsed heating and the power dissipation. An elliptical profile of the iris with large aperture (diameter of 18 mm) has been also implemented to reduce the peak electric field, to increase the frequency separation with the nearest $\pi/2$-mode thus avoiding excitation of this mode with short rf pulses and to have a better pumping on the cathode cell. A four-port mode launcher [10, 11] with an on-axis coupling has been also adopted to reduce the pulsed heating on the coupler and to have a perfect compensation of the dipole and quadrupole field components. The mode launcher has been also designed to integrate two pumping ports. The e.m. design has been done with ANSYS [12] and the e.m. model is reported in Fig. 1 with the magnitude of the electric field. The final gun parameters are given in Table 1.
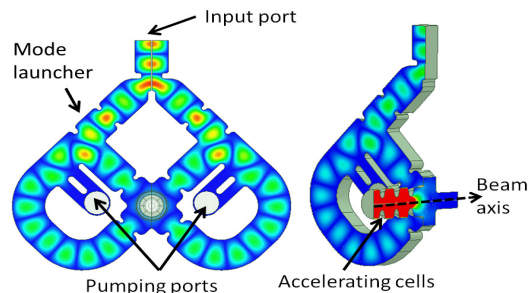
Figure 1: electromagnetic model of the gun.

Table 1: Main Parameters of the C-band Gun

Parameter	value
Resonant frequency	5.712
$E_{cath}/\sqrt{P_{diss}}$ [MV/(m·MW$^{0.5}$)]	51.4
rf input power [MW]	18
Cathode peak field [MV/m]	160
Rep. rate [Hz]	100 (400)
Quality factor	11900
Filling time [ns]	166
Coupling coefficient	3
rf pulse length [ns]	300
Mode sep. π-$\pi/2$ [MHz]	47
E_{surf}/E_{cath}	0.96
Mod. Poy. vector [W/μm^2]	2.5
Pulsed heating [ºC]	16
Average diss. Power [W]	250 (1000)

13th Int. Particle Acc. Conf.

IPAC2022, Bangkok, Thailand

JACoW Publishing

ISBN: 978-3-95450-227-1

ISSN: 2673-5490

doi:10.18429/JACoW-IPAC2022-MOPOMS021

The gun main dimensions and the magnitude and phase of the longitudinal electric field on axis are reported in Figs. 2 and 3 respectively. This last plot put in evidence that the accelerating field is a perfect standing wave in the accelerating cells while, in the coupler region it has a residual travelling wave component (non-constant phase) related to the power flow from the input coupler circular waveguide into the structure. The effect of these travelling wave components on the beam dynamics has been carefully studied also in the case of long circular waveguides [13] and does not affect the beam dynamics.
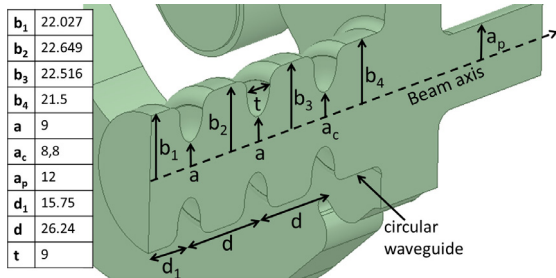
Figure 2: gun main dimensions.
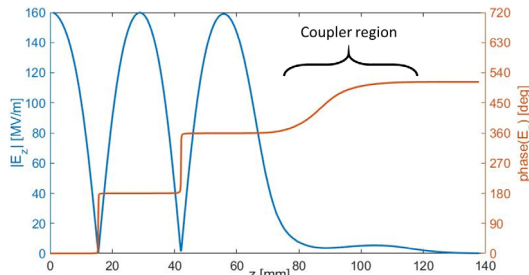
Figure 3: longitudinal electric field on axis.

The magnitude of the magnetic field on three different arcs, with radius 5 mm, in the mode launcher region, is reported in Fig. 4. The arcs are in the center of the mode launcher itself (corresponding to the z=100 mm longitudinal position of Fig. 3), in the center of the circular waveguide (z=80 mm) and at the beginning of the output beam pipe (z=120 mm).
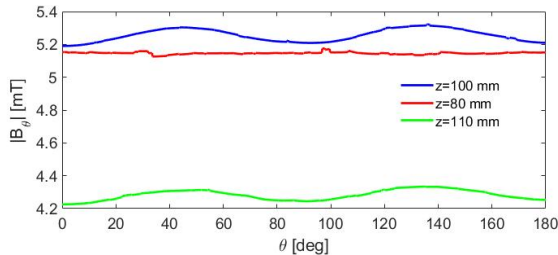
Figure 4: magnetic field on three arcs (r=5 mm) in the mode launcher region.

The plot put in evidence that the residual quadrupole component is completely negligible while there is an octupole component that vanishes moving toward the circular waveguide. Moreover, for a given arc, it is possible to verify that the phase of the field is constant and, for this reason, it is possible to perform a spatial Fourier analysis, according to the formula [14]:

$$B_{\vartheta}(r,\vartheta,z) \cong A_o(z)r + \sum_{n=1}^{\infty} A_n(z)e^{j\phi_n(z)}\cos(n\vartheta)r^{n-1}$$

where the A_n terms are the magnitude of the multipole components. The quadrupole component is that associated to the term with n=2 while the octupole to the term n=4. Their values, in the center of the coupler, are $3.5 \cdot 10^{-4}$ T/m and 400 T/m^3 respectively. Beam dynamics simulations [13], considering also the effect of these multipole components, have shown that their effects on the beam parameters are completely negligible.

THERMO-MECHANICAL DESIGN

The gun will be realized with the new brazing-free technology developed at INFN-LNF [15] and already adopted for the realization of new rf photo-guns [16,17]. This technology has been demonstrated to exhibit very good performances in term of breakdown rates (BDR) and conditioning time, with a contemporary reduction of the cost and realization time. The 3D mechanical layout is given in Fig. 5. In the figure there are also reported the other components to operate the gun such as the pumping system, the solenoid and the laser injection chamber that allows the laser injection with the last mirror in air. The solenoid is a single coil device with a length of 12 cm and a bore radius of 30 mm.
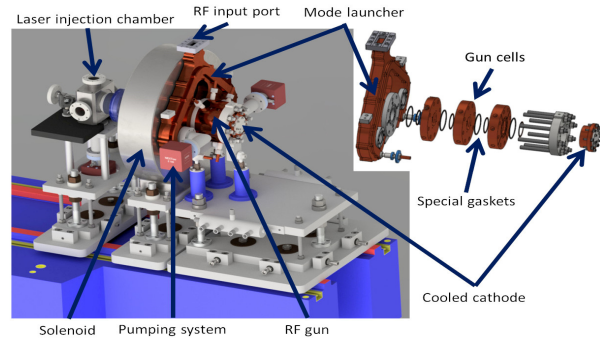
Figure 5: 3D mechanical layout of the gun.

The operation at 100 Hz with 300 ns rf pulses results in an average dissipated power into the gun body of ~250 W. As already pointed out, the gun has been designed also to operate with a higher repetition rate compatible, for example, with the 400 Hz operation now under consideration for the EUPRAXIA@SPARC_LAB project. In this case the dissipated power in the gun is ~1 kW. For this reason, a careful design of the cooling system has been performed to avoid detuning of the gun during operation, and not uniform deformations with a consequence unbalance of the accelerating field in the cells. The gun integrates four cooling channels, as given in Fig. 6a: three for the cells (with internal diameter of 7 mm) and one for the cathode (with a square section ~100 mm^2). In each cooling pipe of the cells it is foreseen a continuous flow of demineralized water of about 2.5 liter/min while for the cathode (because of the larger cooling pipe section) a flow rate of 5 liter/min. The 3D model of the gun, including the cooling system, has been implemented in ANSYS Workbench environment [12] and a full coupled thermal,

structural and electromagnetic analysis, has been performed. The heat load obtained by the e.m. analysis has been imported in the thermo-mechanical module, the temperature distribution has been calculated and the mechanical deformations have been then calculated. The water temperature of the cooling pipes in the 400 Hz operation and the final temperature distribution are given in Figs. 6a and 6b and the corresponding deformations are depicted in Fig. 6c. In the calculations we have considered an input water temperature, and corresponding nominal gun temperature, of 22 °C. The deformed structure has then been simulated with the e.m. module and the calculated detuning is of ~1 MHz while we verified that the field distribution is not affected. The reflection coefficients at the input port, under powering, are reported in Fig. 7 for the 100 Hz and 400 Hz cases and are compared with the nominal one. The plot clearly shows the resonance frequency variation due to the cavity deformation. This detuning can be either compensated by changing the water temperature during powering or by designing the structure with a resonant frequency higher than the nominal one.
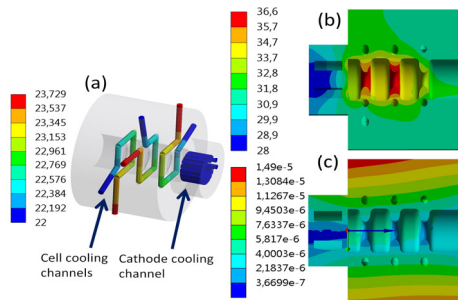
Figure 6: gun cooling system (a); (b) temperature distribution (at 400 Hz) and mechanical deformations (c).
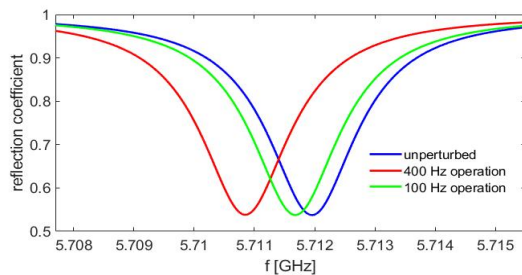
Figure 7: reflection coefficient under powering.

To deeply investigate the gun properties, simulations of the dark current have been also performed using the CST code [18] and are described in detail in [19]. These simulations are important for the radioprotection point of view and high power test stand setup. The calculated charge per period at the laser injection chamber at 160 MV/m with a β enhancement factor of 70 is of 15 fC with a total maximum charge on the rf pulse length well below the 25 pC level.

GUN PROTOTYPE

The realization technology without brazing allows to assemble the gun with special gaskets in a clean room and to proceed, after the vacuum test, directly to the rf characterization. Prior to the final realization of the gun an aluminum prototype has been fabricated and tested at low power. Pictures of the gun under assembly and under rf test are given in Fig. 8. Measurements of the reflection at the input port and electric field with the bead drop technique have also been performed and are reported in Fig. 9. The first measurements showed a detuning of the cathode cell of about 500 kHz and a consequent reduction of the amplitude of the electric field. This has been found to be related to an error in the realization of the cathode cell with a diameter larger than the nominal one of ~20 μm. In the final gun now under realization this error will be corrected.
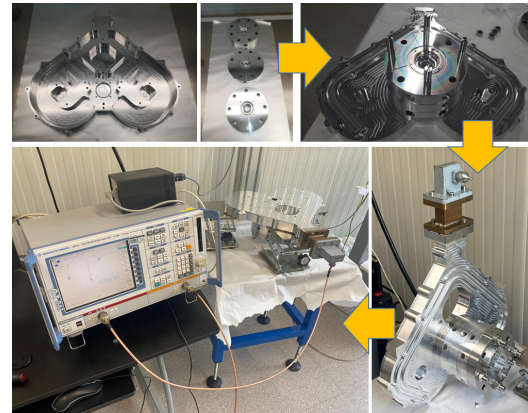
Figure 8: gun assembly and under rf test.
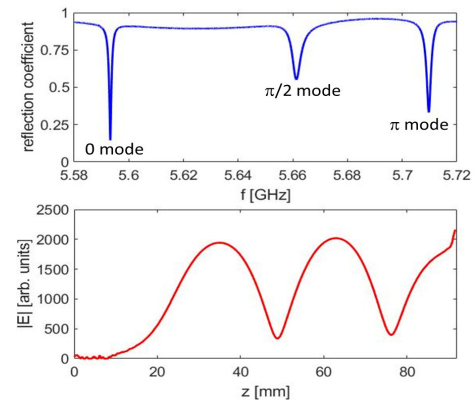
Figure 9: Measurements of the reflection coefficient at the input port (up) and electric field (down).

CONCLUSIONS

A new 2.5 cell C band gun has been designed and will be realized and tested. It integrates a four-port mode launcher, and it has been designed to operate with short rf pulses (300 ns) and cathode peak field larger than 160 MV/m. In the paper we have presented the e.m. and thermo-mechanical design and the rf measurements on an aluminum prototype.

ACKNOWLEDGEMENTS

REFERENCES

[1] M. Ferrario *et al*., "EuPRAXIA@SPARC_LAB Design study towards a compact FEL facility at LNF", arXiv:1801.08717.

[2] http://www.compactlight.eu/Main/HomePage

[3] J.B. Rosenzweig, E. Colby, "Charge and Wavelength Scaling of RF Photoinjector Design", TESLA-95-04, 1995.

[4] V.A. Dolgashev, *et al.,* "RF breakdown in normal conducting single-cell structures", in *Proc. PAC'05*, May 16–20, Knoxville, Tennessee, U.S.A. 2005.

[5] https://ifast-project.eu/home

[6] S. Bettoni, private communications.

[7] D. Alesini *et al.,* "Design of a full C-Band Injector for ultra-high brightness electron beam", in *Proc. IPAC'19*, Melbourne, Australia, May 2019, pp. 1979-1982 doi:10.18429/JACoW-IPAC2019-TUPTS024

[8] A.Grudiev, et al., "New local field quantity describing the high gradient limit of accelerating structures", *Phys. Rev. ST Accel. Beams,* vol. 12, p. 102001, Oct. 2009. doi:10.1103/PhysRevSTAB.12.102001

[9] V. A. Dolgashev, "High Magnetic Field in Couplers of X-Band Accelerating Structures", in *Proc. PAC'03*, pp. 1267-1269. doi:10.1109/PAC.2003.1289674

[10] G. Castorina *et al*., "A TM01 mode launcher with quadrupole field components cancellation for high brightness applications", *J. Phys.: Conf. Ser.* Vol. 1067, p. 082025. doi:10.1088/1742-6596/1067/8/082025

[11] Giuseppe Pedrocchi *et al*., "A C-Band RF Mode Launcher with Quadrupole Field Components cancellation for high brightness applications", in *Proc. IPAC21,* Campinas, SP, Brazil, May 2021, p. 3638. doi:10.18429/JACoW-IPAC2021-WEPAB398

[12] https://www.ansys.com/

[13] A. Giribono *et al.,* "Effects of mode launcher on Beam dynamics in next generation high brightness c-band guns", in *Proc. IPAC'21*, Campinas, SP, Brazil, May 2021, pp. 813-816. doi:10.18429/JACoW-IPAC2021-MOPAB257

[14] D. Alesini *et al.,* "Design of high gradient, high repetition rate damped C-band rf structures", *Phys. Rev. Accel. Beams*, vol. 20, p. 032004, 2017. doi:10.1103/PhysRevAccelBeams.20.032004

[15] D. Alesini *et al.,* International Patent Publication No. WO 2016/147118 A1, assigned to INFN.

[16] D. Alesini *et al.,* "New technology based on clamping for high gradient radio frequency photogun", *Phys. Rev. ST Accel. Beams* vol. 18, p. 092001, 2015. doi:10.1103/PhysRevSTAB.18.092001

[17] D. Alesini *et al*., "Design, realization, and high power test of high gradient, high repetition rate brazing-free S-band photogun", *Phys. Rev. Accel. Beams,* vol. 21, p. 112001, 2018. doi:10.1103/PhysRevAccelBeams.21.112001

[18] https://www.3ds.com/

[19] F. Cardelli *et al.,* "Dark Current Studies for a High Gradient SW C-Band RF Gun", presented at IPAC'22, Bangkok, Thailand, June 2022, paper MOPOMS020, this conference.

[20] http://www.comeb.it/